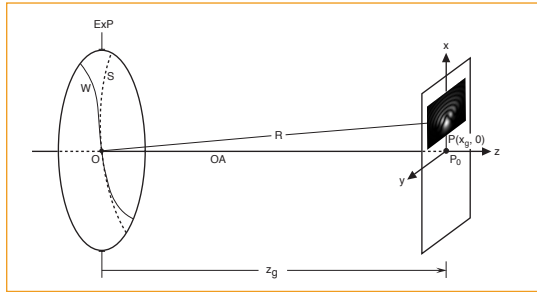


Optical Imaging and Aberrations



© Virendra N. Mahajan

Adjunct Professor
College of Optical Sciences
University of Arizona

The Aerospace Corporation
El Segundo, California 90245
(310) 336-1783

virendra.n.mahajan@aero.org

Imaging Through Atmospheric Turbulence

1

Imaging Through Atmospheric Turbulence

- In ground-based astronomy, a plane wave of uniform amplitude and phase representing the light from a star is incident on the atmosphere.
- As the wave propagates through the atmosphere, it undergoes both amplitude and phase variations due to the random inhomogeneities of the refractive index of air.
- In *near-field imaging* ($L \ll D^2/\lambda$), turbulence primarily introduces aberrations, and a short exposure image provides a better resolution.
- In *far-field imaging* ($L \gg D^2/\lambda$), turbulence introduces not only aberrations but also amplitude variations (called scintillations).
- Wavefront gets distorted, i.e., it becomes nonplanar with nonuniform amplitude across it, and the distortions vary randomly with time.

* Distorted wavefront of nonuniform amplitude is incident on a ground-based imaging system.

3

Summary

Imaging Through Atmospheric Turbulence

- Long Exposure Image
- Mutual Coherence Function and Wave Structure Function
- Atmospheric Coherence Length
- MTF Reduction Factor
- Phase Aberration in Terms of Zernike Polynomials
- Short Exposure Image
- Adaptive Optics

2

Long-Exposure Image

- **Pupil function of the overall system** (i.e., including the effects of atmospheric turbulence) representing the wavefront at the exit pupil:

$$P(\vec{r}_p) = P_L(\vec{r}_p) P_R(\vec{r}_p)$$

- Instantaneous irradiance distribution of the star image formed by the overall system:

$$I_i(\vec{r}_i) = \frac{P_{ex}}{S_{ex} \lambda^2 R^2} \left| \int P(\vec{r}_p) \exp\left(-\frac{2\pi i}{\lambda R} \vec{r}_p \cdot \vec{r}_i\right) d\vec{r}_p \right|^2$$

- Time-averaged PSF:

$$\langle I_i(\vec{r}_i) \rangle = \frac{\langle P_{ex} \rangle}{S_{ex} \lambda^2 R^2} \iint P_L(\vec{r}_p) P_L^*(\vec{r}_p') \langle P_R(\vec{r}_p) P_R^*(\vec{r}_p') \rangle \exp\left[-\frac{2\pi i}{\lambda R} (\vec{r}_p - \vec{r}_p') \cdot \vec{r}_i\right] d\vec{r}_p d\vec{r}_p'$$

- **Mutual coherence function:**

$$\langle P_R(\vec{r}_p) P_R^*(\vec{r}_p') \rangle = \exp\left[-\frac{1}{2} \mathcal{D}_w(|\vec{r}_p - \vec{r}_p'|)\right]$$

4

• **Kolmogorov turbulence:**

$$\mathcal{D}_w(r) = 6.88(r/r_0)^{5/3} \quad (5-83) \quad (\text{Wave structure function})$$

$$r_0 = 0.1847\lambda^{1.2} \left\{ \int_0^L C_n^2(z) (z/L)^{5/3} dz \right\}^{-0.6} \quad (5-84)$$

• r_0 is a characteristic length of turbulence representing its *coherence length* or *diameter*, called **Fried's coherence length**.

• If the line of sight makes an angle θ with the zenith, then the path length L through turbulence increases by $\sec\theta$, or r_0 decreases by $(\sec\theta)^{0.6}$.

$$\mathcal{D}_n(\vec{r}_1, \vec{r}_2) = \langle [n(\vec{r}_1) - n(\vec{r}_2)]^2 \rangle = C_n^2 r^{2/3}, \quad r = |\vec{r}_1 - \vec{r}_2|$$

• Since the refractive index structure parameter C_n^2 at a given site decreases with altitude, the integral in Eq. (5-84) has a higher numerical value when observing a space object from ground (looking upwards) than when observing a ground object from space (looking downwards).

5

• Because of a Fourier transform relationship between the PSF and the OTF, we identify $(\vec{r}_p - \vec{r}_p')/\lambda R$ with a spatial frequency \vec{v}_i :

$$\vec{r}_p - \vec{r}_p' = \lambda R \vec{v}_i$$

• Substituting and carrying out the integration over \vec{r}_p :

$$\langle I_i(\vec{r}_i) \rangle = \langle P_{ex} \rangle \int \tau_L(\vec{v}_i) \exp\left[-\frac{1}{2} \mathcal{D}_w(\lambda R v_i)\right] \exp(-2\pi i \vec{v}_i \cdot \vec{r}_i) d\vec{v}_i$$

$$\tau_L(\vec{v}_i) = S_{ex}^{-1} \int P_L(\vec{r}_p) P_L^*(\vec{r}_p - \lambda R \vec{v}_i) d\vec{r}_p \quad (\text{Turbulence-free OTF})$$

• Using normalized quantities:

$$I(r) = I_i(\vec{r}_i)/I(0), \quad \vec{r} = \vec{r}_i/\lambda F \quad \text{and} \quad \vec{v}_i = \vec{v}/\lambda F, \quad I(0) = \langle P_{ex} \rangle S_{ex}/\lambda^2 R^2$$

$$\therefore \langle I(\vec{r}) \rangle = (4/\pi) \int \langle \tau(\vec{v}) \rangle \exp(-2\pi i \vec{v} \cdot \vec{r}) d\vec{v} \quad (\text{Time-averaged PSF})$$

$$\langle \tau(\vec{v}) \rangle = \tau_L(\vec{v}) \exp\left[-\frac{1}{2} \mathcal{D}_w(vD)\right] \quad (\text{Time-averaged OTF})$$

7

• Correspondingly, r_0 is smaller when a satellite is observed from ground compared to when a ground object is observed from a satellite.

• Consequently, image degradation is much smaller when a ground object is observed from space than when a space object is observed from ground.

• In the first case, the object is near the region of turbulence and it is observed from far away. In the second case, the object is away from the region of turbulence, but it is observed from nearby.

• This is similar to when an object behind a diffuse shower glass is observed. One can see some detail in the object when it is in contact with the shower glass. However, as soon as the object is moved slightly away from the shower glass, it appears only as a halo, illustrating complete loss of image resolution.

• *Reciprocity* of wave propagation does hold. That is why wavefront errors of a wave from a point source in space can be corrected with a deformable mirror on ground yielding a diffraction limited (neglecting any measurement or correction error) beam in space.

6

• MCF for Kolmogorov turbulence:

$$\langle P_R(\vec{r}_p) P_R^*(\vec{r}_p') \rangle = \exp\left[-\frac{1}{2} \mathcal{D}_w(r)\right] = \exp\left[-3.44(r/r_0)^{5/3}\right]$$

• Time-averaged OTF of the overall system:

$$\langle \tau(\vec{v}; D/r_0) \rangle = \tau_L(\vec{v}) \exp\left[-\frac{1}{2} \mathcal{D}_w(vD)\right] = \tau_L(\vec{v}) \langle \tau_a(v; D/r_0) \rangle$$

$$\langle \tau_a(v; D/r_0) \rangle = \exp\left[-3.44(vD/r_0)^{5/3}\right] = \exp\left[-3.44(v_i \lambda R/r_0)^{5/3}\right] \quad (5-94)$$

• $\langle \tau_a(v; D/r_0) \rangle$ is the **long-exposure MTF reduction factor** associated with atmospheric turbulence.

• $\langle \tau_a \rangle$ is independent of the pupil diameter D , as it should be.

8

- Since $\exp(-3.44) \simeq 0.03$, atmospheric turbulence reduces the overall system MTF for a spatial frequency $\nu = r_0/D$ by a factor of 0.03.

- Since $\langle \tau_a \rangle$ represents the *mutual irradiance function* of the wave, its magnitude describes the *degree of spatial coherence* of the wave, and thus the visibility of fringes formed in a Young's two-pinhole experiment.

- Hence, r_0 represents a *spatial coherence length* of the wave so that its degree of coherence corresponding to two points on it separated by r_0 is 0.03, or that the visibility of the fringes formed by the secondary waves from these points is only 0.03.

9

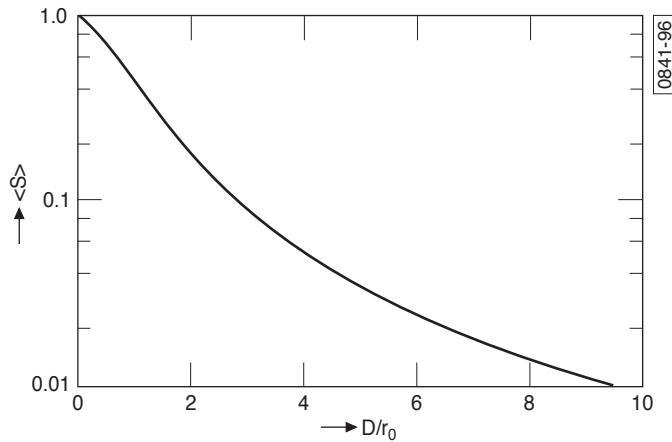


Figure 5-6b. Time-averaged Strehl ratio.

- Strehl ratio decreases to zero monotonically as D/r_0 increases.
- For a given value of D , Strehl ratio decreases rapidly as r_0 decreases.
- Even when r_0 is as large as D , the Strehl ratio is only 0.445.

11

Application to Circular Pupils

- Assume that the turbulence-free system is aberration free with uniform transmittance.

- Time-averaged PSF of the overall system:

$$\langle I(r; D/r_0) \rangle = 8 \int_0^1 \langle \tau(\nu; D/r_0) \rangle J_0(2\pi r \nu) \nu d\nu$$

$$\langle \tau(\nu; D/r_0) \rangle = \tau_L(\nu) \exp[-3.44(\nu D/r_0)^{5/3}]$$

$$\tau_L(\nu) = \frac{2}{\pi} \left[\cos^{-1} \nu - \nu(1 - \nu^2)^{1/2} \right], \quad 0 \leq \nu \leq 1$$

- Time-averaged Strehl ratio:

$$\langle S(D/r_0) \rangle = \langle I(0; D/r_0) \rangle = 8 \int_0^1 \langle \tau(\nu; D/r_0) \rangle \nu d\nu$$

10

- Unnormalized time-averaged central irradiance:

$$\langle I_i(0; D/r_0) \rangle = \frac{\langle P_{ex} \rangle S_{ex}}{\lambda^2 R^2} \langle S(D/r_0) \rangle = \frac{\langle P_{ex} \rangle S_a}{\lambda^2 R^2} \eta(D/r_0)$$

- $S_a = \pi r_0^2/4$ is the *coherent area* of the atmosphere.

$$\eta(D/r_0) = (D/r_0)^2 \langle S(D/r_0) \rangle = 8 \left(\frac{D}{r_0} \right)^2 \int_0^1 \tau_L(\nu) \exp[-3.44(\nu D/r_0)^{5/3}] \nu d\nu \quad (5-99)$$

- Whereas the Strehl ratio represents the central irradiance normalized by its aberration-free value, η represents the central irradiance normalized by the aberration-free value when the pupil diameter is r_0 .

12

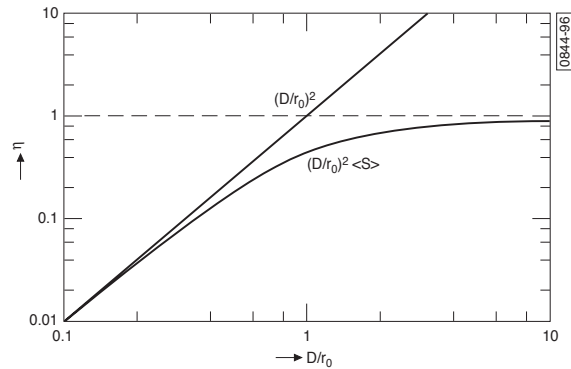


Figure 5-6c. Time-averaged central irradiance for a fixed total power represented by η .

- Aberration-free value of η increases as $(D/r_0)^2$, as illustrated by the straight line.
- For small values of D/r_0 , aberrated value of η also varies as $(D/r_0)^2$. As D increases, η increases much more slowly with a negligible increase for $D/r_0 > 5$.

13

• Purpose of a *large* ground-based telescope has therefore generally not been better resolution (before the advent of *adaptive optics*) but to collect more light so that dim objects may be observed.

• In the case of a laser transmitter with a fixed value of laser power P_{ex} , the central irradiance on a target will again be limited to its aberration-free value for an exit pupil of diameter r_0 , no matter how large the transmitter diameter D is.

15

Limiting performance

• In astronomical observations, $\langle P_{ex} \rangle$ increases as D increases. However, if the observation is made against a uniform background, then the background irradiance in the image also increases with D as D^2 .

• Hence, the detectability of a point object is limited by turbulence to a value corresponding to an exit pupil of diameter r_0 , no matter how large the diameter D of the exit pupil is.

• At visible wavelengths, $r_0 \simeq 10$ cm. Consequently, the performance of a ground-based telescope making astronomical observations in the visible region is limited primarily by atmospheric turbulence to a telescope of diameter $D \simeq 10$ cm.

14

Phase Aberration in Terms of Zernike Circle Polynomials

• So far, we have calculated performance degradation by propagation through atmospheric turbulence without any knowledge of the phase aberrations introduced by it.

• Now we expand the phase aberration introduced by atmospheric turbulence in terms of orthonormal Zernike circle polynomials $Z_j(\rho, \theta)$:

$$\Phi(\rho, \theta) = \sum_j a_j Z_j(\rho, \theta)$$

• **Circle polynomials** may be written:

$$Z_{\text{even } j}(\rho, \theta) = \sqrt{2(n+1)} R_n^m(\rho) \cos m\theta, \quad m \neq 0$$

$$Z_{\text{odd } j}(\rho, \theta) = \sqrt{2(n+1)} R_n^m(\rho) \sin m\theta, \quad m \neq 0$$

$$Z_j(\rho, \theta) = \sqrt{n+1} R_n^0(\rho), \quad m = 0, \quad j \text{ is even or odd depending on the value of } n$$

16

• Polynomials varying as $\sin m\theta$ are also included here, since the turbulent atmosphere does not have an axis of rotational symmetry.

• Index j is a *polynomial-ordering number* and is a function of both n and m .

• Polynomial number ordering:

• Polynomial with a lower value of n is ordered first.

• For a given value of n , a polynomial with a lower value of m is ordered first.

• Even j corresponds to a symmetric polynomial varying as $\cos m\theta$

• Odd j corresponds to an antisymmetric polynomial varying as $\sin m\theta$.

• When $m = 0$, j may be even or odd depending on the value of n .

j	n	m	$Z_j(\rho, \theta)$
13	4	2	$\sqrt{10}(4\rho^4 - 3\rho^2)\sin 2\theta$
14	4	4	$\sqrt{10}\rho^4 \cos 4\theta$
15	4	4	$\sqrt{10}\rho^4 \sin 4\theta$
16	5	1	$\sqrt{12}(10\rho^5 - 12\rho^3 + 3\rho)\cos \theta$
17	5	1	$\sqrt{12}(10\rho^5 - 12\rho^3 + 3\rho)\sin \theta$
18	5	3	$\sqrt{12}(5\rho^5 - 4\rho^3)\cos 3\theta$
19	5	3	$\sqrt{12}(5\rho^5 - 4\rho^3)\sin 3\theta$
20	5	5	$\sqrt{12}\rho^5 \cos 5\theta$
21	5	5	$\sqrt{12}\rho^5 \sin 5\theta$
22	6	0	$\sqrt{7}(20\rho^6 - 30\rho^4 + 12\rho^2 - 1)$
23	6	2	$\sqrt{14}(15\rho^6 - 20\rho^4 + 6\rho^2)\sin 2\theta$
24	6	2	$\sqrt{14}(15\rho^6 - 20\rho^4 + 6\rho^2)\cos 2\theta$

Table 5-4. Orthonormal Zernike *circle* polynomials $Z_j(\rho, \theta)$.

j	n	m	$Z_j(\rho, \theta)$
1	0	0	1
2	1	1	$2\rho \cos \theta$
3	1	1	$2\rho \sin \theta$
4	2	0	$\sqrt{3}(2\rho^2 - 1)$
5	2	2	$\sqrt{6}\rho^2 \sin 2\theta$
6	2	2	$\sqrt{6}\rho^2 \cos 2\theta$
7	3	1	$\sqrt{8}(3\rho^3 - 2\rho)\sin \theta$
8	3	1	$\sqrt{8}(3\rho^3 - 2\rho)\cos \theta$
9	3	3	$\sqrt{8}\rho^3 \sin 3\theta$
10	3	3	$\sqrt{8}\rho^3 \cos 3\theta$
11	4	0	$\sqrt{5}(6\rho^4 - 6\rho^2 + 1)$
12	4	2	$\sqrt{10}(4\rho^4 - 3\rho^2)\cos 2\theta$

25	6	4	$\sqrt{14}(6\rho^6 - 5\rho^4)\sin 4\theta$
26	6	4	$\sqrt{14}(6\rho^6 - 5\rho^4)\cos 4\theta$
27	6	6	$\sqrt{14}\rho^6 \sin 6\theta$
28	6	6	$\sqrt{14}\rho^6 \cos 6\theta$
29	7	1	$4(35\rho^7 - 60\rho^5 + 30\rho^3 - 4\rho)\sin \theta$
30	7	1	$4(35\rho^7 - 60\rho^5 + 30\rho^3 - 4\rho)\cos \theta$
31	7	3	$4(21\rho^7 - 30\rho^5 + 10\rho^3)\sin 3\theta$
32	7	3	$4(21\rho^7 - 30\rho^5 + 10\rho^3)\cos 3\theta$
33	7	5	$4(7\rho^7 - 6\rho^5)\sin 5\theta$
34	7	5	$4(7\rho^7 - 6\rho^5)\cos 5\theta$
35	7	7	$4\rho^7 \sin 7\theta$
36	7	7	$4\rho^7 \cos 7\theta$
37	8	0	$3(70\rho^8 - 140\rho^6 + 90\rho^4 - 20\rho^2 + 1)$

Correlation of Zernike Coefficients

- Orthonormality of Zernike polynomials

$$\int_0^1 \int_0^{2\pi} Z_j(\rho, \theta) Z_{j'}(\rho, \theta) \rho d\rho d\theta \bigg/ \int_0^1 \int_0^{2\pi} \rho d\rho d\theta = \delta_{jj'}$$

- Expansion coefficients:

$$a_j = \pi^{-1} \int \Phi(\rho, \theta) Z_j(\rho, \theta) \rho d\rho d\theta$$

- **Cross correlation** of the expansion coefficients:

$$\begin{aligned} \langle a_j^* a_{j'} \rangle &= \left(1/\pi^2\right) \int d\bar{\rho} \int d\bar{\rho}' Z_j^*(\bar{\rho}) Z_{j'}(\bar{\rho}') \langle \Phi(\bar{\rho}) \Phi(\bar{\rho}') \rangle \\ &= \left(1/\pi^2\right) \int d\bar{\rho} \int d\bar{\rho}' Z_j^*(\bar{\rho}) Z_{j'}(\bar{\rho}') R_\Phi(|\bar{\rho} - \bar{\rho}'|) \end{aligned}$$

21

Table 5-5. Correlation of Zernike polynomial expansion coefficients for **near-field** propagation in units of $(D/r_0)^{5/3}$.

Correlation Coefficient Pairs	Zernike Order		Correlation Value
	n	n'	$\langle a_j a_{j'} \rangle$
a_2^2, a_3^2	1	1	4.49×10^{-1}
a_4^2, a_5^2, a_6^2	2	2	2.32×10^{-2}
$a_2 a_8, a_3 a_7$	1	3	1.42×10^{-2}
$a_7^2, a_8^2, a_9^2, a_{10}^2$	3	3	6.19×10^{-3}
$a_4 a_{11}, a_5 a_{13}, a_6 a_{12}$	2	4	3.88×10^{-3}
$a_{11}^2, a_{12}^2, a_{13}^2, a_{14}^2, a_{15}^2$	4	4	2.45×10^{-3}
$a_7 a_{17}, a_8 a_{16}, a_9 a_{19}, a_{10} a_{18}$	3	5	1.56×10^{-3}
$a_{16}^2, a_{17}^2, a_{18}^2, a_{19}^2, a_{20}^2, a_{21}^2$	5	5	1.19×10^{-3}
$a_{11} a_{22}, a_{12} a_{24}, a_{13} a_{23}, a_{14} a_{26}, a_{15} a_{25}$	4	6	7.60×10^{-4}

23

- Zernike coefficients are not statistically independent.

- For a given value of n , the crosscorrelations (and, therefore, autocorrelations) do not depend on the value of m .

- For a given value of n , the correlation values decrease rapidly as the order difference $n' - n$ increases.

- First nonzero cross-correlations are $\langle a_2 a_8 \rangle$ and $\langle a_3 a_7 \rangle$, i.e., the tilt-coma cross-correlations.

22

Table 5-6. Correlation of Zernike polynomial expansion coefficients for **near-field** propagation in units of $(D/r_0)^{5/3}$ for $n=1$ and $n' \geq 1$.

Correlation Coefficient Pairs	Zernike Order		Order Difference	Correlation Value
	n	n'	$n' - n$	$\langle a_j a_{j'} \rangle$
a_2^2, a_3^2	1	1	0	4.49×10^{-1}
$a_2 a_8, a_3 a_7$	1	3	2	1.42×10^{-2}
$a_2 a_{16}, a_3 a_{17}$	1	5	4	7.54×10^{-4}
$a_2 a_{30}, a_3 a_{29}$	1	7	6	-9.52×10^{-6}
$a_2 a_{46}, a_3 a_{47}$	1	9	8	8.61×10^{-7}
$a_2 a_{68}, a_3 a_{67}$	1	11	10	-1.41×10^{-7}
$a_2 a_{92}, a_3 a_{93}$	1	13	12	3.24×10^{-8}
$a_2 a_{122}, a_3 a_{121}$	1	15	14	-9.29×10^{-9}
$a_2 a_{154}, a_3 a_{155}$	1	17	16	3.14×10^{-9}

24

Modal correction and residual error

- Residual aberration variance when the first J modes are corrected:

$$\Delta_J = \pi^{-1} \int_0^1 \int_0^{2\pi} \left\langle \left[\Phi(\rho, \theta) - \sum_{j=1}^J a_j Z_j(\rho, \theta) \right]^2 \right\rangle \rho d\rho d\theta$$

$$= \langle \Phi^2 \rangle - \langle a_1^2 \rangle - \sum_{j=2}^J \langle a_j^2 \rangle = \Delta_1 - \sum_{j=2}^J \langle a_j^2 \rangle$$

- No correction:

$$\Delta_1 \equiv \sigma_\Phi^2 = 1.03(D/r_0)^{5/3}$$

- Since $r_0 \sim \lambda^{1.2}$, variance of the wave aberration is independent of λ , as expected in the absence of atmospheric dispersion.

- x and y tilts corrected (short exposure image):

$$\Delta_3 = 0.134(D/r_0)^{5/3}$$

- Tilt-corrected variance is reduced by a factor of $1.03/0.134 \simeq 7.7$.

25

Strehl Ratio

Long-exposure image

- $\exp(-\sigma_\Phi^2)$ is not a good approximation for estimating the Strehl ratio:

$$\langle S_1(D/r_0) \rangle = \exp(-\sigma_\Phi^2) \simeq \exp[-1.03(D/r_0)^{5/3}]$$

- Even for a small value of $D/r_0 = 1$, $\langle S_1 \rangle = 0.357$, compared to a true value of 0.445.

- $\langle S_1 \rangle$ underestimates the Strehl ratio more and more as D/r_0 increases.

- Much better approximation (yielding a slight overestimation):

$$\langle S_2(D/r_0) \rangle \simeq [1 + (D/r_0)^{5/3}]^{-1.2}$$

27

Table 5-7. Variance of residual phase errors for **near-field** propagation in units of $(D/r_0)^{5/3}$.

$\Delta_1 = 1.0299$	$\Delta_{12} = 0.0352$
$\Delta_2 = 0.582$	$\Delta_{13} = 0.0328$
$\Delta_3 = 0.134$	$\Delta_{14} = 0.0304$
$\Delta_4 = 0.111$	$\Delta_{15} = 0.0279$
$\Delta_5 = 0.0880$	$\Delta_{16} = 0.0267$
$\Delta_6 = 0.0648$	$\Delta_{17} = 0.0255$
$\Delta_7 = 0.0587$	$\Delta_{18} = 0.0243$
$\Delta_8 = 0.0525$	$\Delta_{19} = 0.0232$
$\Delta_9 = 0.0463$	$\Delta_{20} = 0.0220$
$\Delta_{10} = 0.0401$	$\Delta_{21} = 0.0208$
$\Delta_{11} = 0.0377$	$\Delta_J \approx 0.2944J^{-\sqrt{3}/2}$ (For large J)

26

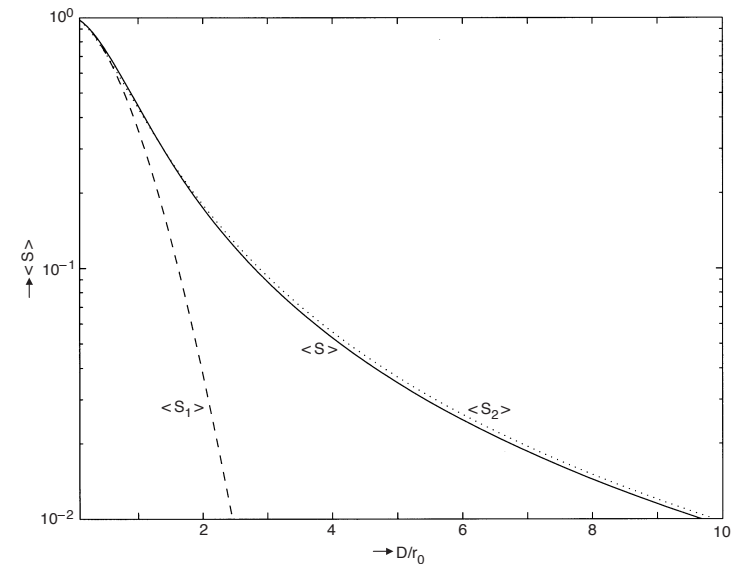


Figure 5-12. Variation of time-averaged Strehl ratio $\langle S \rangle$ with D/r_0 .

28

Short-Exposure Image

- A time-averaged short-exposure image is obtained if the tilt is corrected in real time, for example, with a steering mirror.

- Short-exposure or tilt-corrected aberration variance:

$$\sigma_{\Phi_{tc}}^2 = 0.134(D/r_0)^{5/3}$$

- $\exp(-\sigma_{\Phi}^2)$ with $\sigma_{\Phi}^2 = 0.134(D/r_0)^{5/3}$ approximates the true value of Strehl ratio reasonably well for $D/r_0 \leq 6$.

- Variance of angle of arrival:

$$\sigma_{\alpha}^2 + \sigma_{\beta}^2 = \left(\frac{3.58\lambda}{\pi D}\right)^2 (D/r_0)^{5/3}$$

29

Random Aberration Example

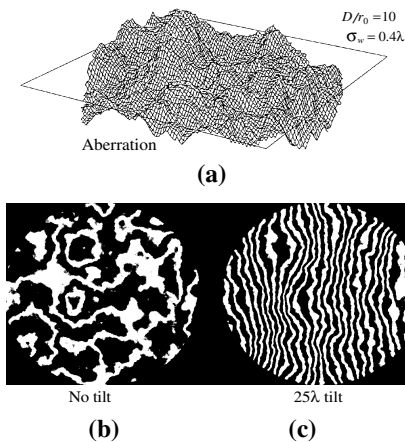


Figure 5-15. Aberration introduced by **atmospheric turbulence** for $D/r_0 = 10$. (a) Aberration shape. (b) Aberration interferogram. (c) Interferogram with 25λ of wavefront tilt.

31

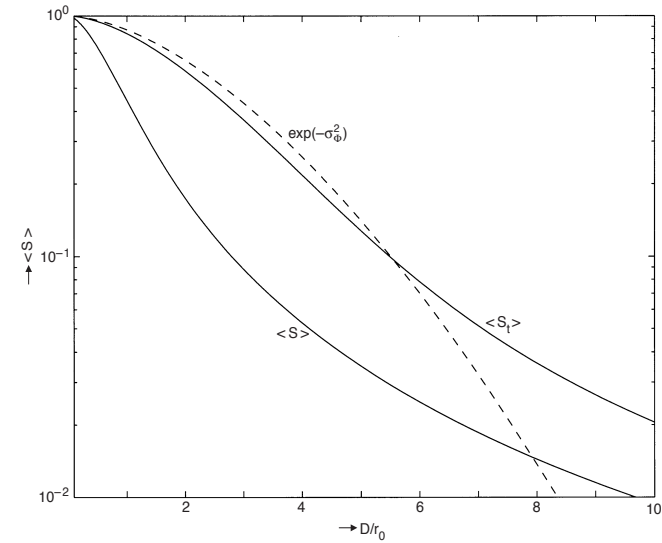
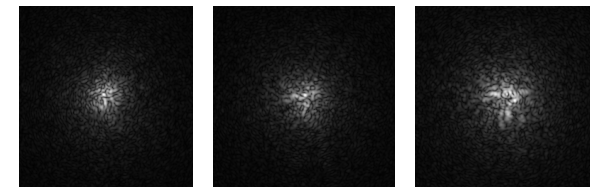


Figure 5-13c. Near-field tilt-corrected time-averaged Strehl ratio $\langle S_t \rangle$. The uncorrected Strehl ratio $\langle S \rangle$ is shown to illustrate the improvement made by tilt correction.

30

Short-Exposure PSFs for $D/r_0 = 10$



- Each image is broken up into small spots called **speckles**, which is a characteristic of random aberrations.

- Angular size of a speckle is approximately equal to λ/D .

- Angular size of the overall image is approximately equal to λ/r_0 .

- For a given value of D , the overall image size increases as r_0 decreases, showing the effects of what astronomers call **seeing**.

- For a given value of r_0 , the image size is approximately constant, but the size of a speckle decreases as D increases. Thus an increase in D , does not significantly improve the resolution of the system (as determined by the overall size of the image).

32

Adaptive Optics

Correction of wavefront errors in (near) real time by using a steering mirror and a deformable mirror is called *adaptive optics*.

- Steering mirror with only three actuators corrects the large x and y wavefront tilts (also called tip and tilt).
- *Deformable mirror* deformed by actuating an array of actuators attached to it corrects the wavefront deformation.
- Actuator signals are independent of the optical wavelength provided atmospheric dispersion is negligible.

Zonal approach

- In the zonal approach, signals for the actuators are determined by sensing the wavefront errors with a wavefront sensor in a closed loop to minimize the variance of the residual errors.
- Zonal approach has the advantage that the rate of correction is limited only by the rate at which the wavefront errors can be sensed and the actuators can be actuated.

33

References

1. D. Fried, "Optical resolution through a randomly inhomogeneous medium for very long and very short exposures," J. Opt. Soc. Am. **56**, 1372–1379 (1966).
2. R. J. Noll, "Zernike polynomials and atmospheric turbulence," J. Opt. Soc. Am. **66**, 207–211 (1976).
3. G.-m Dai and V. N. Mahajan. "Zernike annular polynomials and atmospheric turbulence," J. Opt. Soc. Am. **A 24**, 139–155 (2007).
4. J. W. Hardy, Adaptive Optics for Astronomical Telescopes, Oxford, New York, (1998).
5. R. K. Tyson, Introduction to Adaptive Optics, SPIE Press, Bellingham, Washington (1999).
6. V. N. Mahajan, J. Govignon, and R. J. Morgan, "Adaptive optics without wavefront sensors," SPIE Proc. Vol 228, *Active Optical Devices and Applications*, 63-69 (1980).

35

- However, the amount of light that is used by the wavefront sensor in sensing the wavefront errors is lost from the image.
- Moreover, for imaging an (isoplanatic) extended object, wavefront sensing requires a point source in its vicinity.

Modal approach

- In the modal approach, the actuators are actuated to produce Zernike modes (e.g., focus, two modes of astigmatism, two modes of coma, etc.) iteratively until image sharpness $\int I^2(\vec{r})d\vec{r}$, where $I(\vec{r})$ is the image irradiance distribution, is maximized.
- In the modal approach, there is no loss of light, but the rate or the bandwidth of correction can be slow due to its iterative nature, especially when turbulence is severe and a large number of modes must be corrected.
- However, no point source is needed, since the modal approach is applicable to the extended object itself.

34